RSC Advances

ROYAL SOCIETY OF CHEMISTRY

www.rsc.org/advances

Journal Name

ARTICLE

Photocytotoxic luminescent lanthanide complexes of DTPA–bisamide using quinoline as photosensitizer

Received 00th January 20xx,
Accepted 00th January 20xx

DOI: 10.1039/x0xx00000x

www.rsc.org/

Khushbu Singh,[a] Samya Banerjee[b] and Ashis K. Patra*[a]

Lanthanide complexes [Ln(DTPAAQ)(DMF)] (**1**-**3**) (Ln = Pr (**1**), Eu (**2**), Tb (**3**), H_3DTPAAQ = *N*,*N*''-Bis(3-amidoquinolyl) diethylenetriamine-*N*,*N*',*N*''-triacetic acid, DMF = *N*,*N*-dimethylformamide were studied for their structures, photophysical properties, DNA and protein binding, DNA photocleavage, photocytotoxicity and cellular internalization. The crystal structures of complexes [Ln(DTPAAQ)(DMF)] (**1**-**3**) displays a discrete mononuclear nine-coordinate {LnN_3O_6} tricapped-trigonal prism (TTP) coordination geometry. The europium and terbium complexes show strong luminescent properties in visible region having long luminescence lifetime (τ = 0.51 – 0.64 ms). The conjugated 3-aminoquinoline moieties act as efficient light harvesting antenna, which upon photoexcitation transfer its energy to Eu(III) or Tb(III) for their characteristic $^5D_0 \rightarrow {}^7F_J$ or $^5D_4 \rightarrow {}^7F_J$ *f*-*f* transitions respectively. The complexes display efficient binding affinity to DNA (K_b = 3.4 x 10^4 – 9.8 x 10^4 M^{-1}) and BSA (K_{BSA} = 3.03 x 10^4 – 6.57 x 10^4 M^{-1}). Europium and terbium complexes gives enhanced luminescence upon interacting with CT-DNA suggesting possible luminescent-based sensing applications for these complexes. Complexes **1**-**3** show moderate cleavage of supercoiled (SC) DNA to its nicked circular (NC) form on exposure to UV-A light of 312 nm involving formation of singlet oxygen ($^1O_2$) and hydroxyl radical ($^{\bullet}OH$) in a type-II and a photoredox pathways. Eu(III) and Tb(III) complexes exhibit remarkable photocytotoxicity with human cervical cancer cell line (HeLa) (IC_{50} = 20.7-28.5 μM) while remain essentially noncytotoxic upto 150 μM in dark. Nontoxic in nature complexes is suitable for designing cellular imaging agents. Fluorescence microscopy data reveal primarily cytosolic localization of the Eu(III) and Tb(III) complexes in HeLa cells.

Introduction

The fascinating luminescence properties of the trivalent lanthanides (Ln) have diverse applications in bioimaging, luminescent probes, sensors, drug delivery, medical diagnosis, MRI, catalysis, labels for biomolecules and stains for cellular imaging.[1-3] The unusual and fascinating optical properties of Ln(III) results from shielding of the *f*-electrons by outer filled *s*- and *p*-electrons. Due to intrinsically weak absorption of Ln(III) ions, it can be coordinated with a chromophore acting as a light harvesting antenna, which then transfer the energy to the excited state of lanthanide ion.[3] Lanthanide complexes have been widely used as luminescent sensors due to their long excited state lifetimes in milliseconds range, large Stokes' shift, favorable excitation and emission wavelengths in biological media, and sharp emission bands distinct from organic flurophores.[2-5] Moreover, the time-gated luminescence measurements from lanthanides having long excited state lifetime is a sensitive and elegant solution to eliminate the interference from the short-lived background autofluorescence from complex biological media including time-resolved immunoassays.[6] Magnetic resonance imaging (MRI) is the most important and prominent non-invasive diagnostic technique used in clinical medicine and biomedical research aided by gadolinium(III)-based contrast agents.[7,8] The Gd(III)-based complexes based on polyaminocarboxylate ligands like $[Gd(DTPA)(H_2O)]^{2-}$ (Magnevist®) and $[Gd(DOTA)(H_2O)]^{-}$ (Dotarem®) are predominant MRI contrast agents in commercial use.

Lanthanides are typically chelated with multidentate chelating ligands which forms stable coordinatively saturated Ln(III) complexes and also protect it from quenching through vibrational energy dissipation for application in luminescence imaging or sensing. Thus designing polydentate ligands incorporated with a sensitizing antenna fluorophore in the same ligand framework established as an important approach to design highly emissive lanthanide based bioprobes for cellular imaging and sensing.[9-13] Recently, a DTPA-bisamide-metronidazole based terbium(III) complex been reported as a luminescent sensor for human serum albumin (HSA) and for specific recognition of DNA depurination sites.[14] Such light-activated photosensitization ability is also important towards designing luminescent photoactivated chemotherapeutic

[a] *Department of Chemistry, Indian Institute of Technology Kanpur, Kanpur 208016, Uttar Pradesh, India. E-mail: akpatra@iitk.ac.in; Tel: +91 512 259 6780*
[b] *Department of Inorganic and Physical Chemistry, Indian Institute of Science, Bangalore 560012, Karnataka, India.*

† Electronic Supplementary Information (ESI) available: ESI-MS spectra; unit cell packing diagrams; selected bond distances and angles; luminescence spectra; DNA and protein binding plots; DNA cleavage; cytotoxicity data. For ESI and crystallographic data in CIF or other electronic format see DOI: 10.1039/x0xx00000x.

agents for their potential utility in the photodynamic therapy (PDT) of cancer.[15,16]

There are several photoactivatable d-block transition metal complexes which were widely explored for their photo-induced DNA damage activities.[17-21] On the contrary, there are only limited reports on lanthanide complexes of texaphyrins and *N*,*N*-donor heterocyclic bases showing photo-induced DNA cleavage activity.[22-25] Chakravarty et al. have recently reported photo-induced DNA cleavage and photocytotoxicity activity of a series of La^{3+} and Gd^{3+} complexes of planar phenanthroline, pyridylphenanthroline and substituted terpyridine bases as photosensitizer with UV-A light.[23] It would be of great interest to develop redox-stable, photobleaching resistant trivalent luminescent and photosensitizable lanthanide complexes for their application as phototherapeutic and time-delayed cellular imaging agents.

The present work stems from our current interest to explore and design stable luminescent lanthanide complexes for cellular imaging and sensing applications.[24] Here we have used a versatile ligand framework based on diethylenetriamine-*N*,*N*',*N*''-pentaacetic acid (DTPA) bisamide conjugated with 3-aminoquinoline (DTPAAQ) as a light-harvesting fluorophore antenna (Scheme 1).

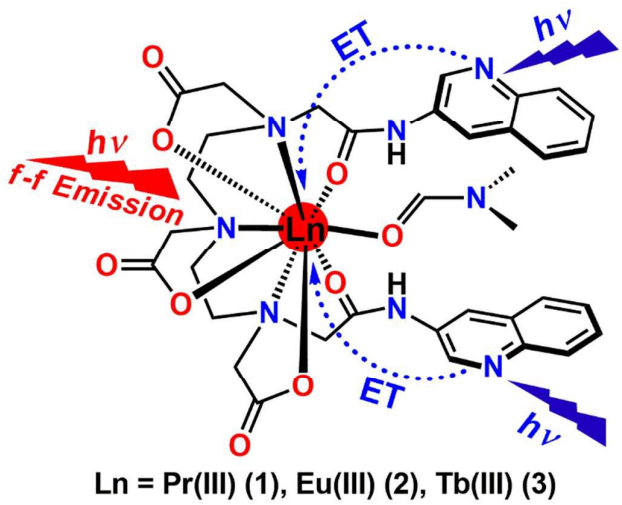

Scheme 1 Schematic presentation of complexes **1**-**3** and antenna moieties showing photosensitization and energy transfer pathway for f-f emission.

Such DTPA-bis(diamide) ligands act as octadentate chelates equipped with hard donors like carboxylates and amides are appropriate considering hard-acid nature of Ln(III) to form thermodynamically stable complexes. The emissive lanthanide complexes derived from quinoline fluorophores conjugated to macrocyclic cyclen ligands with longer excitation wavelength were reported for their uses in *'on-off'*-based pH sensing, luminescent molecular logic gates, selective anion sensing applications.[25,26] Such appended fluorophore to the DTPA ligand enable us to study the cellular internalization of the complexes by confocal fluorescence microscopy. We have chosen emissive Eu(III) and Tb(III) ions in the visible region possessing long emission lifetimes. Moreover, the redox stability of trivalent lanthanide complexes is highly desirable for cellular applications in presence endogenous reducing agents like thiols (GSH, metallothionines) and ascorbates. The presence of photoactive quinoline moiety in the complexes is likely to show the photocytotoxicity which could make them suitable for phototherapeutic applications. Attempts have been made to explore the structural features, luminescence properties, biological interactions and activities of the complexes.

Herein, we report the synthesis, molecular structures, photophysical properties, DNA and protein binding, photo-induced DNA cleavage activity, photocytotoxicity and cellular internalization of the lanthanide(III) complexes [Ln(DTPAAQ)(DMF)] (**1**-**3**) (Ln = Pr(III) (**1**), Eu(III) (**2**), Tb(III) (**3**), H_3DTPAAQ = *N*,*N*''-Bis(3-amidoquinolyl)diethylenetriamine-*N*,*N*',*N*''-triacetic acid) (Scheme 1). Complexes **1**-**3** were structurally characterized by X-ray crystallography showing nine-coordinate $\{LnN_3O_6\}$ TTP coordination geometry. They demonstrate potential binding propensity with DNA in aqueous medium and Eu(III) and Tb(III) complexes show significant enhancement of luminescence intensity in presence of DNA via inhibiting nonradiative relaxation processes. The Eu and Tb-complexes show photo-induced DNA cleavage and efficient photocytotoxicity in UV-A light, while remain noncytotoxic in dark. The complexes **2** and **3** show cellular internalization and cytosolic localization as evidenced from their intrinsic luminescence using confocal fluorescence imaging studies with HeLa cells.

Results and discussion

Synthesis and general aspects

H_3DTPAAQ was synthesized from the acylation reaction between DTPA bis(anhydride) and 3-aminoquinoline in DMF in good yield and purity. The ligand was characterized thoroughly by ^{1}H and ^{13}C-NMR, ESI-MS, FT-IR and UV-Vis spectroscopy. UV-vis absorption spectrum of the ligand in DMF displays a structured and broad absorbance band ranging from 260-332 nm due to π-π* electronic transitions in the ligand. FT-IR data show ~20-30 cm^{-1} shift to lower frequency for $\nu_{C=O}$ of –CONH and ~60-70 cm^{-1} for $-CO_2^-$ groups from free ligand upon complexation with Ln(III) ion which is consistent with the coordination through carboxylate and amide oxygen. H_3DTPAAQ ligand shows a broad emission band ($S_1 \rightarrow S_0$) at 411 nm upon excitation at 260 nm. The complexes [Ln(DTPAAQ)(DMF)] (**1**-**3**) are synthesized in 70-85% yield by a general synthetic procedure via the addition of the deprotonated ligand to the corresponding chloride or nitrate salts of the lanthanides in 1:1 molar ratio in water (Scheme S1, ESI†) and recrystallized from layering a DMF solution of complexes with Et_2O. All the complexes have been characterized by elemental analysis, electrospray ionization mass spectrometry (ESI-MS), FT-IR, UV-visible, emission spectral studies and structurally characterized by X-ray crystallography. The crystal structures of the complexes **1**-**3** reveals coordinatively saturated octadentate DTPAAQ ligand

and a bound DMF ligand in the coordination sphere as they were grown from DMF solution. Complexes show structural integrity in solution as evidenced

Complex	IR (cm^{-1})[a]			(λ/nm)(ε/$M^{-1}cm^{-1}$) [b]	Λ_M/(Scm^2M^{-1})[c]	K_b/M^{-1}[d]	K_{app}/M^{-1}[e]	K_{BSA}/M^{-1}[f]
	$\nu_{asym}(CO_2)$	$\nu_{sym}(CO_2)$	$\nu_{C=O}$(CONH)					
1	1609	1388	1588	263 (10200); 318 (5000); 331 (5200)	13.6	(9.8 ± 0.6) x 10^4	1.19 x 10^4	(3.03±0.4) x 10^4
2	1607	1388	1589	263 (17300); 318 (5040) 331 (5020)	11.8	(3.4± 0.3) x 10^4	8.08 x 10^5	(3.35±0.3) x 10^4
3	1609	1393	1589	263 (13000); 318 (6000) 331 (7000)	17.2	(3.6 ±0.2) x 10^4	1.14 x 10^4	(6.573±0.5) x 10^4

Table 1. Selected physicochemical, DNA and BSA binding parameters for [Ln(DTPAAQ)(DMF)] (**1**-**3**)

[a]IR stretching frequency in KBr phase. [b]UV electronic spectral bands in DMF. [c]Λ_M, molar conductivity in S cm^2 M^{-1} in 10% aqueous DMF at 25 °C. [d]K_b, intrinsic DNA binding constant with calf thymus DNA. [e]Apparent DNA binding constant determined from ethidium bromide displacement assay. [f] Stern-Volmer fluorescent quenching constant determined from tryptophan fluorescent quenching in BSA.

from molecular ion peaks with matching isotopic distribution profile in mass spectral data in solution (Figs S1-S3 in ESI†). Selected physicochemical data for the complexes were given in Table 1. The electronic absorption spectra of the complexes in aqueous-DMF exhibit well-defined ligand centered $S_0 \rightarrow S_1$ and $S_0 \rightarrow S_2$ π-π* electronic transitions centered at ~325 nm and ~260 nm respectively.[26] Absorption spectral profile of the complexes **1**-**3** are independent of the nature of the lanthanide ion and matches well with the free H_3DTPAAQ ligand. This clearly indicates that overall energy transfer takes place from the remote quinoline moieties of the ligand to the Ln(III). The molar conductivity values for the complexes suggest non-electrolytic nature of the complexes in aqueous DMF which supports neutral character of the complexes in solution.

X-Ray crystallography

X-ray quality single crystals of complexes **1**-**3** were obtained by layering of diethyl ether on to a DMF solution of the complexes at room temperature. The molecular structures of [Pr(DTPAAQ)(DMF)]·DMF·$4H_2O$ (**1**·DMF·$4H_2O$), [Pr(DTPAAQ)(H_2O)] (**1a**), [Eu(DTPAAQ)(DMF)]·$4H_2O$ (**2**·$4H_2O$) and [Tb(DTPAAQ)(DMF)]·DMF·$3H_2O$ (**3**·DMF·$3H_2O$), were established by single crystal X-ray diffraction studies. Complexes **1** and **1a** crystallized in the $P2_1/c$ and $P\bar{1}$ space groups of the monoclinic and triclinic crystal systems with four and two molecules in the unit cell respectively.

Complex **1a** essentially having identical structure to complex **1** except ninth site is occupied by the oxygen atom of a bound water instead of DMF (Figs S5, S6 in ESI†). Complexes **2** and **3** crystallized in the $P2_1/n$ space group with four molecules in the unit cell. The ORTEP views of the complexes **1-3** with the atom numbering scheme is shown in Fig. 1 and selected structural parameters and refinement details are listed in Table S1, ESI†. Unit cell packing diagrams are shown in Figs S4, S6-S8 and selected bond lengths and angles are listed in Tables S2-S5 in ESI†.

All the [Ln(DTPAAQ)(Solv)] (**1a**, **1**-**3**) (Ln = Pr (**1, 1a**); Eu (**2**); Tb (**3**); Solv = H_2O (**1a**); DMF (**1**, **2** and **3**)) complexes are discrete mononuclear species with the Ln(III) centre in a nine-coordinate {LnN_3O_6} distorted tricapped-trigonal prism (TTP) coordination geometry. Such TTP coordination polyhedron are reported in literature for related DTPA-based Gd(III), Lu (III) and Yb (III) complexes.[27,28] The octadentate chelating ligand ($DTPAAQ^{3-}$) coordinates the lanthanide ion through three amine nitrogens, three carboxylate oxygens and two amide oxygens, and the ninth site is occupied by the oxygen atom of a DMF or a water molecule. The two triangular faces of the trigonal prism are constituted by O1, O2, O5 and O3, O4, N2, respectively, while N1, N3 and O6 of the terminal amines and coordinated DMF or H_2O are in the capping position of three rectangular faces. The Ln(III) is located close the centre of the trigonal prism and Ln-O_{solv} bond is almost perpendicular to the rectangular mean plane to which it's capped. A description of the coordination polyhedra of the complexes were shown in Figs 1d and S9, ESI†.

The Ln-O_{DMF} bond length decreases from **1** to **3** which corresponds to the decreasing atomic radius of the Ln(III) and ranges from 2.453(4) Å to 2.358(3) Å. A similar expected decrease in bond lengths were also observed in other Ln-O and Ln-N bonds in **1**-**3** (Fig. S10 in ESI†). Ln-O_{amide} bond length ranges from 2.513(4) Å to 2.441(3) Å and Ln-$O_{carboxylate}$ bond distance ranges from 2.415(4) Å to 2.333 (3) Å respectively. Ln-$N_{terminal}$ bond lengths ranges from 2.780(5) Å to 2.695(4) Å whereas Ln-$N_{central}$ bond lengths ranges from 2.697(4) Å to 2.625(4) Å. On average Ln-N bond distances are ~0.3 Å longer than the Ln-O distances indicative of the lower bond strength of the less polar Ln-N bonds, compared to the Ln-O ionic bonds. The geometry and variation of such bond lengths have been also observed earlier for the other related DTPA-derived complexes of Gd, Lu and Yb.[29,30]

Photophysical properties

Measurement of steady state emission spectra of the complexes **1-3** in aqueous-DMF (9:1 v/v) at 298 K shows

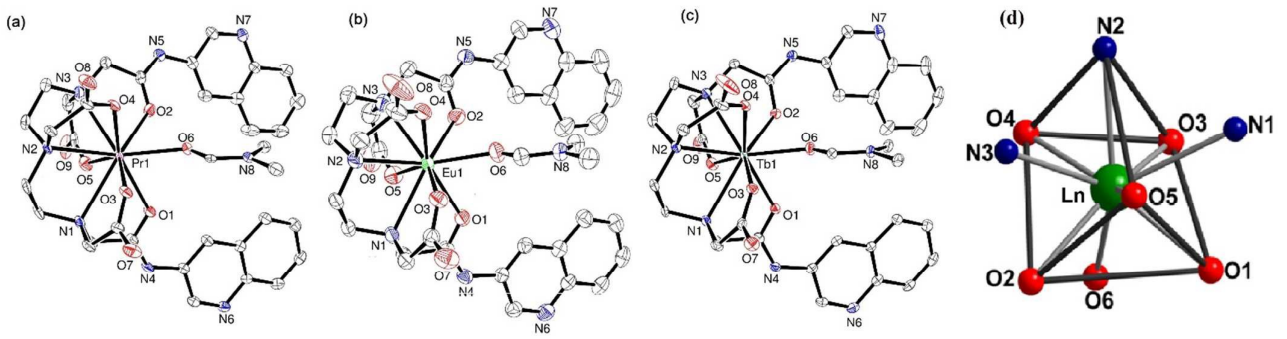

Fig. 1 ORTEP views of [Ln(DTPAAQ)(DMF)] (**1**-**3**) (Ln = Pr (**1**), Eu (**2**), Tb (**3**)) (a-c) with with 50% probability thermal ellipsoid with atom labelling schemes for the metal and heteroatoms. Coordination polyhedra of the nine-coordinate $\{LnN_3O_6\}$ lanthanide cores showing tricapped-trigonal prism (TTP) coordination geometry in complexes **1-3** (d).

predominant radiative relaxation through quinoline based DTPAAQ ligand fluorescence centred at ~350 nm followed by emission bands from emissive lanthanide excited states (Fig. S11, ESI†). Eu(III) and Tb(III) complexes with long excited state luminescence lifetimes in milliseconds range are ideally suitable for time-gated luminescence imaging applications.[8] Luminescence spectral studies with a time delay were performed to avoid rapid short-lived ligand fluorescence from quinoline groups. [Eu(DTPAAQ)(DMF)] (**2**) shows characteristic europium based red luminescence on excitation at 330 nm attributed to the $^5D_0 \rightarrow {}^7F_J$ *f-f* transitions of Eu(III) (J = 0–4) and (Fig. 2).

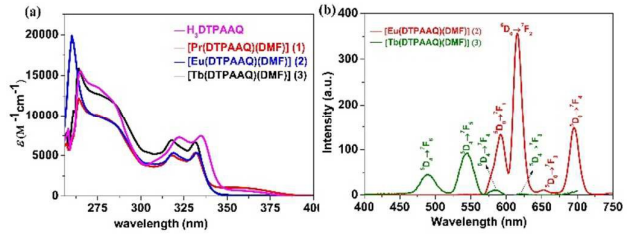

Fig. 2 (a) UV-visible spectra of H_3DTPAAQ ligand and [Ln(DTPAAQ)(DMF)] (**1**-**3**) complexes in aqueous-DMF (9:1 v/v) at 298 K. (b) The time-resolved luminescence spectra of [Eu(DTPAAQ)(DMF)] (**2**) and [Tb(DTPAAQ)(DMF)] (**3**) in aqueous DMF (9:1 v/v) at 298 K. Delay time = 0.1 ms, λ_{ex} = 330 nm, slit width = 5 nm.

The most intense band at 616 nm originated from electric dipole (ED) induced hypersensitive $^5D_0 \rightarrow {}^7F_2$ transition. The emission spectra of [Tb(DTPAAQ)(DMF)](**3**) shows characteristic Tb(III)green luminescence correspond to the $^5D_4 \rightarrow {}^7F_J$ *f-f* transitions (J = 6-3). The emission spectra of [Pr(DTPAAQ)(DMF)] (**1**) shows low intensity non-discernible Pr(III) emission in the visible region (450-750 nm) typical for $^3P_0 \rightarrow {}^3H_J$ or ^3F_J *f-f* transitions of Pr(III) suggesting poor ligand to Pr(III) energy transfer or non-radiative quenching (Fig. S11, ESI†). The emissive excited state lifetimes (τ) were determined from the emission decay profile for the complexes **2** (τ = 0.64 ms) and **3** (τ = 0.51 ms) in aqueous media at 298 K. Typical decay profiles and mono-exponential curve fittings are given in Fig. 3. The overall luminescence quantum yields ($\phi_{overall}$) for complexes **1**-**3** were 0.018, 0.036 and 0.021 respectively.

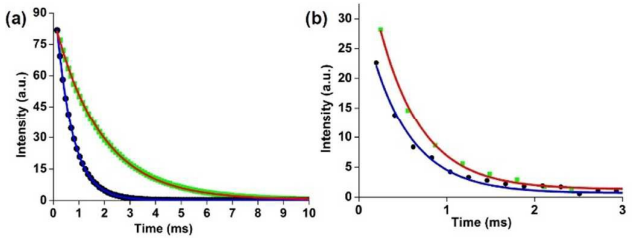

Fig. 3 Luminescence lifetime measured for (a) [Eu(DTPAAQ)(DMF)] (**2**) and (b) [Tb(DTPAAQ)(DMF)] (**3**) from decay profile for excited state $^5D_0$ and $^5D_4$ at 616 nm and 543 nm respectively in H_2O and D_2O under ambient condition at T= 298 K, λ_{ex} = 330 nm, [complex] = 40 μM, delay and gate time = 0.1 ms, total decay time = 0.1 ms, Ex. and Em. slit = 10 nm. Red and blue curves are single exponential fitting curve in D_2O and H_2O respectively.

The higher quantum yield for Eu-complex could be ascribed to ideally placed triplet energy state of quinoline sensitizer for efficient energy transfer to the comparatively lower energy $^5D_0$ emissive excited state of Eu(III).[29]

In case of Tb(III) the smaller energy gap between chromophore triplet state and excited emissive states of Tb(III) leads back energy transfer to the quinoline triplet state alongwith possible quenching by oxygen lead to lower quantum yield. Coordination of water molecules lowers the excited-state lifetime of Ln(III) through nonradiative quenching via high-frequency O-H oscillator. In aqueous media, the complexes undergo exchange of bound DMF by water. To understand this phenomena, we have determined the number of inner-sphere water molecules (q) of the complexes in solution by measuring luminescence lifetimes in H_2O and D_2O via modified Horrock's equation.[30] The determined hydration numbers (q ~1) were in agreement with displacement of one DMF molecule by one water molecule in aqueous media. The luminescence spectra of complexes **1-3** clearly demonstrates that light-harvesting quinoline moiety upon photoexcitation transfers it's energy to the excited ^5D_J state of the lanthanide through antenna effect.

DNA binding studies

DNA is the most important pharmacological target for numerous metal-based chemotherapeutic drugs. Therefore, we investigated the DNA-binding propensity of the lanthanide complexes using various spectroscopic techniques. The binding properties of the lanthanide complexes **1**-**3** with calf-thymus DNA (CT-DNA) were studied by electronic absorption spectral titrations (Fig. 4). Bathochromic shift and hypochromism is attributed to intercalative mode of binding due to perturbation of π orbitals of DNA base pairs with the π orbitals of the intercalated ligand.[31] The absorption spectral traces of complex **3** with increasing concentration of CT-DNA is shown in Fig. 4a. The intrinsic DNA binding constants (K_b) of the complexes were obtained by monitoring the changes in absorbance of the complexes with increasing DNA concentrations (Figs S14-S16, ESI†).[32] The calculated K_b values for complexes **1**-**3** are in the range of 3.4 x 10^4 – 9.8 x 10^4 M^{-1} suggesting good binding propensity with CT-DNA through two planner quinoline moieties as observed in a hairpin-shaped heterometallic luminescent Ln-Pt_2 complexes.[33]

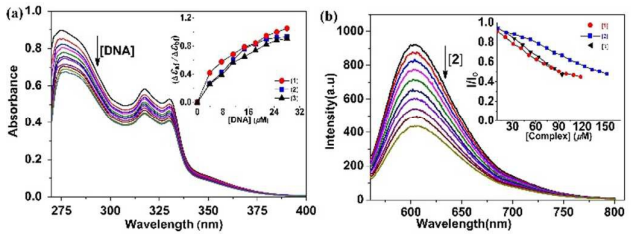

Fig. 4 (a) Absorption spectral traces of the complex **3** on addition of CT-DNA in Tris-HCl/NaCl buffer medium (5 mM, pH 7.2) at 298 K. The inset shows the plot of $\Delta\varepsilon_{af}/\Delta\varepsilon_{bf}$ *vs.* [DNA] for the complexes **1**-**3**. (b) Fluorescence spectral traces of the CT-DNA bound ethidium bromide (EB) (3.0 μM) in 5 mM Tris-HCl/NaCl buffer (pH 7.2) in the presence of increasing concentration of [Eu(DTPAAQ)(DMF)] (**2**) at 298 K. Inset shows plot of relative fluorescence emission intensity (I/I_0) at λ_{em} = 601 nm (λ_{ex} = 546 nm) of EB bound DNA with increasing concentrations of complexes **1**-**3**.

The ethidium bromide (EB) displacement assay is an effective fluorescence spectral technique to investigate relative binding interaction of metal complexes with double stranded CT-DNA. The binding of complexes **1**-**3** to the CT-DNA has been studied using the emission intensity of EB-bound to DNA as a spectral probe. EB is non-emissive in a Tris-HCl buffer medium, however shows intense fluorescence when bound to ds-DNA due to its strong intercalation between the adjacent DNA base pairs. The displacement of EB by titration with the complex solution leads to decrease in the emission intensity of EB at 601 nm due to competitive binding of the lanthanide complexes to the CT-DNA (Fig. 4b, Figs S17-S19, ESI†). The extent of decrease in fluorescence intensity gives a measure of the relative binding affinity of the complexes towards CT-DNA. The apparent binding constant (K_{app}) was calculated using the equation:[34] K_{EB}[EB] = K_{app}[complex], where [complex] is the concentration of the complex at a 50% reduction of fluorescence intensity of EB and K_{EB} = 1 x 10^7 M^{-1}, [EB] =3.0 μM. The calculated K_{app} for complexes **1**-**3** are in the range of 1.14 x 10^4 – 8.08 x 10^5 M^{-1} suggesting a partial intercalative and/or groove binding nature of the complexes.

BSA binding studies

Serum albumin proteins constitute major part of total plasma proteins and plays a crucial role in in the drug transport and metabolism. Interaction of the complexes **1**-**3** with bovine serum albumin (BSA), a structural homolog with human serum albumin (HSA) was studied using quenching of intrinsic tryptophan fluorescence of BSA.[35] Intrinsic fluorescence of BSA is due to the presence of two tryptophan residues (Trp-134 and Trp-212) in a hydrophobic environment. The fluorescence intensity of BSA centered at 345 nm decreases steadily with gradual increase of concentration of the complexes **1**-**3**. The significant quenching of emission intensity possibly results from various molecular interactions arises due to perturbation of BSA secondary structure upon binding of the lanthanide complexes including subunit association, protein denaturation, substrate binding, or conformation changes of the protein.[36] The Stern-Volmer quenching constant for BSA fluorescence (K_{BSA}) for complexes **1**-**3** have been calculated with the Stern-Volmer equation[35] and corresponding Stern-Volmer plots (Figs S20, S21, ESI†) and listed in Table 1. The K_{BSA} values of ~10^4 M^{-1} indicate that the complexes favourably bind to serum proteins thus possibly may enhances the transport and release of protein-bound complexes through biological fluids at cellular level.

DNA sensing application

The time-gated luminescence measurements with luminescent europium and terbium complexes having sharp distinguishable emission bands, long luminescence lifetimes have been successfully employed as luminescent bioprobes for diverse applications in sensing and detection.[4,6] The time-resolved luminescence spectra of complexes **2** and **3** in the presence of increasing CT-DNA concentration were studied in Tris-HCl/NaCl buffer (Fig. 5, Fig. S22 in ESI†). Upon increasing CT-DNA concentration, the intensity of all the characteristic emission bands originating from $^5D_0 \rightarrow {}^7F_J$ (J = 0-4) for Eu(III) and $^5D_4 \rightarrow {}^7F_J$ (J = 6-3) for Tb(III) significantly enhanced. The most prominent changes in emission intensity observed for the electric dipole induced hypersensitive peak at 616 nm (ΔJ = 2) for europium complex **2** and the band at 543 nm (ΔJ = 1) for terbium complex **3**. We have observed a 5-fold enhancement of emission intensity at 615 nm for Eu(III) complex in presence of 2 equiv. of CT-DNA.

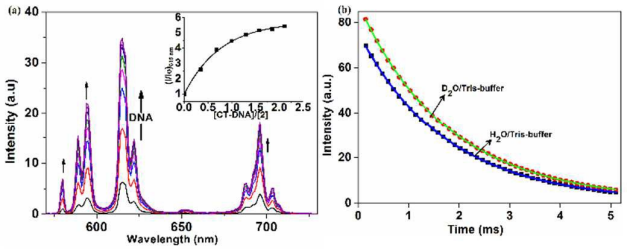

Fig. 5 (a) The time-resolved luminescence spectra of complex **2** (400 μM, λ_{ex} = 330 nm) upon addition of increasing the quantity of calf-thymus DNA in buffer(5 mM Tris-HCl/NaCl, pH 7.2) medium at 298 K. The inset shows the relative emission intensity at 615 nm *vs.* the [CT-DNA]/[**2**] ratio. (b) Luminescence decay profile from $^5D_0$ state of Eu(III) in complex **2** at λ_{em} = 616 nm (λ_{ex} = 330 nm) in presence of CT-DNA in 5 mM Tris buffer in water (blue) and in D_2O (green). [**2**] = 40 μM, [DNA] = 60 μM, delay time and

gate time = 0.1 ms, Ex. and Em. slit = 10 nm. The solid lines are the best fits considering single-exponential behaviour of the decay.

The enhancement of luminescence intensity possibly ascribed to the displacement of the lanthanide coordinated H_2O in DNA-bound state and thereby minimising the nonradiative quenching through O-H oscillators and enhances lifetime of excited emissive sates of Eu(III) or Tb(III) (Figs 5b, S23, ESI†).This is also evident from appreciably lower hydration number (*q*) for the complexes determined in presence of CT-DNA (see SI). DNA may interact through negatively charged phosphate oxygen or by intercalation and alter the primary coordination around Ln(III).[37] Similar observations were reported earlier in literature in terms of application of luminescent lanthanide probes for nucleic acids and protiens as sensors or structural probes.[37,38]

Photo-activated DNA cleavage studies

Photo-induced DNA cleavage activity of the complexes **1**-**3** was studied using supercoiled pUC19 DNA (0.2 μg, 30 μM) in Tris-HCl/NaCl (50 mM, pH 7.2) buffer on irradiation with a low power monochromatic UV light of 312 nm (8W) (Fig. 6a).

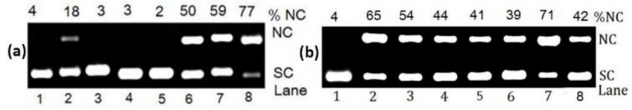

Fig. 6 (a) Cleavage of SC pUC19 DNA (0.2 μg, 30 μM) by the complexes **1**-**3** (100 μM) in 50 mM Tris-HCl/NaCl buffer (pH, 7.2) containing 10% DMF on photoirradiation at 312 nm for 40 min: lane 1, DNA control; lane 2, DNA + H_3DTPAAQ; lane 3, DNA + **1** (in dark); lane 4, DNA + **2** (in dark), lane 5, DNA + **3** (in dark); lane 6, DNA + **1**; lane 7, DNA + **2**; lane 8, DNA + **3**. (b) Photo-induced DNA cleavage activity of complex **2** (100 μM) in the presence of different additives at 312 nm (8 W) for an exposure time of 40 min: lane 1, DNA control; lane 2, DNA + **2**; lane 3, DNA + L-histidine (0.2 mM) + **2**; lane 4, DNA + NaN_3 (0.2 mM) + **2**; lane 5, DNA + KI (0.2 mM) + **2**; lane 6, DNA + DMSO (2 μL) + **2**; lane 7, DNA + D_2O (16 μL) + **2**; lane 8, DNA + catalase (4 U) + **2**.

All the complexes show photoinduced DNA cleavage activity in micromolar complex concentration. The complexes **1** and **2** show ~70% and complex **3** show ~90% cleavage of SC DNA to its nicked circular (NC) form on photoirradiation at 312 nm with a complex concentration of 100 μM for 1 h. The extent of photocleavage of SC-DNA to NC form increases with exposure time or with increasing complex concentrations (Fig. S24, ESI†). The control experiments with only SC DNA alone or SC-DNA with the ligands and lanthanide salts do not show any significant cleavage activity under similar experimental conditions. The complexes remain cleavage inactive in dark condition, thus preclude possibility of any hydrolytic cleavage. UV-light induced DNA cleavage activity of complexes **1**-**3** containing DTPAAQ ligand is likely to involve photosensitization of appended planar aromatic quinoline moiety as a remote photosensitizer that could generate triplet photo excited states which in turn transfer energy to ground state triplet oxygen ($^3O_2$) to form reactive oxygen species effecting DNA cleavage through an oxidative pathway.[39] The energy transfer efficiency from quinoline sensitizer to Tb(III) is less efficient due to less energy gap between the T_1 state of the quinoline sensitizer and $^5D_4$ luminescent level of Tb(III) and thermally-promoted back-transfer of energy from $^5D_4$ to the T_1 excited state of the ligand. Actually this process works in favour for non-radiative energy transfer to triplet ground state of dioxygen($^3\Sigma_g^-$, $^3O_2$) for generating potential reactive oxygen species ($^1O_2$,$^\bullet$OH).[29]

The mechanistic aspects of the photo-induced DNA cleavage reactions of the complexes **1**-**3** have been studied through a series of experiments using reagents like sodium azide and L-histidine as singlet oxygen quenchers; DMSO, catalase and KI as hydroxyl radical scavengers (Fig. 6b). Addition of singlet oxygen quenchers like NaN_3 and L-histidine partially inhibits the photo-induced DNA cleavage activity, whereas hydroxyl radical scavengers like DMSO, KI or catalase also show moderate inhibition in photo-induced DNA cleavage. The formation of $^1O_2$ is also evidenced from the enhanced photcleavage activity in D_2O because of longer lifetime of $^1O_2$ than that in water.[40] These results is suggestive towards involvement of both $^1O_2$ and $^\bullet$OH radicals as cleavage active reactive oxygen species involving both type-II and photoredox pathways respectively and in conformity with earlier reports.[23,24]

Cell cytotoxicity

Cytotoxicity of the Eu and Tb complexes was studied on human cervical cancer cell line (HeLa) under the darkness and upon photo-exposure with the UV-A light of 365 nm using MTT assay.[19b] The complexes, upon prior incubation for 8 h in the dark and subsequent photo-exposure to UV-A light of 365 nm for 30 min, showed decrease in the cell viability giving respective IC_{50} values of 20.7±1.1 μM for Eu complex and 28.5±0.7 μM for Tb complex in light while remain essentially

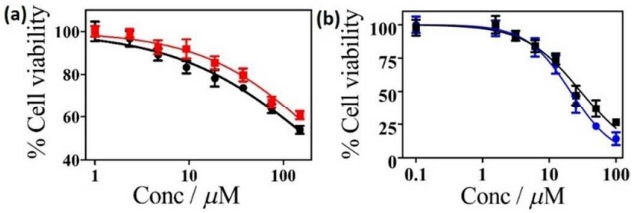

Fig. 7 (a) Cytotoxicity of the complexes **2** (■) and **3** (●) in HeLa cell lines on 8 h incubation in dark as determined by MTT assay. (b) Cytotoxicity of the Eu (●) and Tb (■) complexes in HeLa cell lines on 8 h incubation in dark followed by exposure to UV-A light of 365 nm (0.55 J cm^{-2}) for 30 min, as determined from the MTT assay.

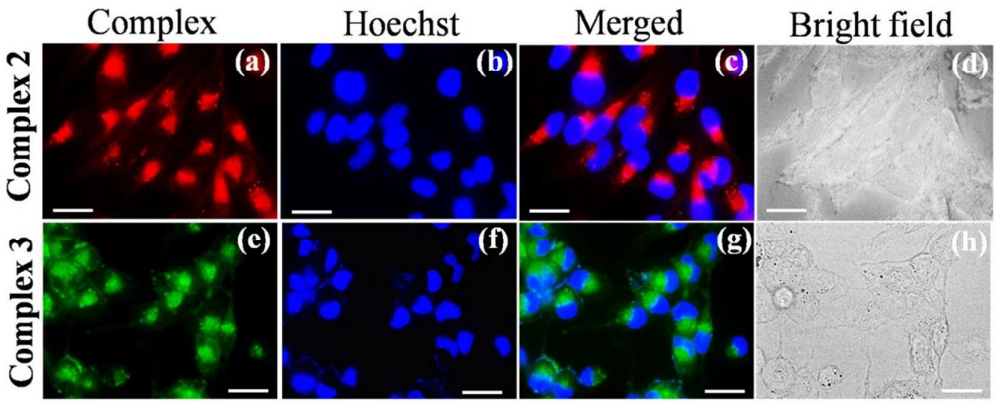

Fig. 8 Fluorescence microscopic images of the HeLa cells treated with complexes **2** and **3** (150 μM) on 8 h incubation and Hoechst 33342 dye (5 μg mL^{-1}): panels (a, e) show red and green emission of complexes **2** and **3** respectively; panels (b, f) show the blue emission of the Hoechst dye staining nucleus; panels (c, g) are the merged images showing cytosolic localization of the complexes; panels (d, h) are respective bright field images., For complex **2**: λ_{ex} = 330 nm, emission filter = LP 585 filter; for complex **3**: λ_{ex} = 330 nm, emission filter = LP 508 filter; scale bar = 20 μM.

nontoxic under darkness even upto a concentration of 150 μM (Fig. 7). Lanthanide complexes of the DTPA–bisamide quinoline ligand are thus remarkably photocytotoxic under UV-A light while remain nontoxic in the dark. The results are indeed remarkable since the complexes could serve the dual purpose of imaging the tumor for its detection and remaining passive within the cells in absence of light and become cytotoxic on photo-irradiation damaging the tumor.

Cellular internalization studies

The long-lived and intrinsic strong emission property of the Eu(III) and Tb(III) complexes was used to study their cellular uptake and localization in HeLa cells by fluorescence microscopy (Fig. 8) Hoechst 33342 was used as a nuclear staining dye to ascertain the intracellular localization of the complexes. The complexes internalized into the HeLa cells and showed significant cellular accumulation within 8 h of incubation. The europium complex showed characteristic red fluorescence whereas the terbium complex showed typical green fluorescence under identical condition [panels (a) and (e)]. The co-staining data with Hoechst 33342 indicate retention of the complexes mainly in the cells cytoplasm [panels (c) and (g)]. A very important question is whether the cells remain viable and healthy over the period of experiment. In answer of this question, the cellular and nuclear morphology were found to remain intact as evident from the microscopy images and bright field images indicating the nontoxic nature of the complexes as confirmed by MTT assay (IC_{50} >150 μM). The results are indeed remarkable considering potential applications for these complexes as cellular imaging agents.

Experimental

Materials

All the reagents and chemicals were purchased from commercial sources (Alfa Aesar, USA; Sigma-Aldrich, U.S.A) and used as such without further purifications. Solvents used were either HPLC grade or were purified by standard procedures.[41] Supercoiled (SC) pUC19 DNA (CsCl purified) was obtained from Merck Millipore (India). Calf thymus DNA (CT-DNA), bovine serum albumin (BSA), ethidium bromide (EB), catalase, agarose (molecular biology grade), gel loading solution, Hoechst 33342 were purchased from Sigma (U.S.A.). Tris-(hydroxymethyl)aminomethane-HCl (Tris-HCl) buffer (pH 7.2) was prepared from Milli-Q water of resistivity of 18.2 MΩ.cm^{-1}.

Measurements

The elemental microanalyses were performed using a Perkin-Elmer 2400 Series II elemental analyzer. FTIR spectra were collected with a Perkin-Elmer Model 1320 FT-IR spectrometer. Electronic spectra were measured at 298 K using a Perkin-Elmer Lambda 25 UV-vis spectrophotometer. ^{1}H-NMR spectra were recorded at 298 K on a JEOL-ECX 500 FT (500 MHz) instrument with chemical shift referenced to tetramethylsilane (TMS = Me_4Si). Electrospray ionization mass spectral (ESI-MS) measurements were carried out using a WATERS Q-TOF Premier mass spectrometer. The fluorescence and time-delayed luminescence spectra were recorded using Agilent Cary eclipse fluorescence spectrophotometer at 298 K. Lifetime measurements for complexes **2** and **3** were done under ambient conditions using a pulsed Xenon lamp at λ_{ex} = 330 nm and λ_{em} = 616 nm and 543 nm for Eu(III) and Tb(III) complexes respectively with a delay time and gate time of 0.1 ms. Decay curves were fitted by non-linear least square method. The overall luminescence quantum yields of the complexes were measured in DMF at room temperature according to a reported procedure using quinine sulfate as reference using following equation:[35]

$$\emptyset_{\text{overall}} = \emptyset_{\text{ref}} \frac{A_{\text{ref}} I n^2}{A I_{\text{ref}} n_{\text{ref}}^2}$$

where *A*, *I* and *n* denote the respective absorbance at the excitation wavelength, area under the emission spectral curve and refractive index of the solvent respectively. The ϕ_{ref}

represents the quantum yield of the standard quinine sulfate solution. The excited state lifetime measurements in water and deuterium oxide allowed the determination of the number of water molecules (q) directly coordinated to the respective lanthanide center using the following modified Horrocks' equations for Eu and Tb respectively.[30]

$$q_{\mathrm{Eu}} = 1.2\left(\frac{1}{\tau_{\mathrm{H_2O}}} - \frac{1}{\tau_{\mathrm{D_2O}}} - 0.25\right)$$

$$q_{\mathrm{Tb}} = 5.0\left(\frac{1}{\tau_{\mathrm{H_2O}}} - \frac{1}{\tau_{\mathrm{D_2O}}} - 0.06\right)$$

Synthesis of *N*,*N*''-Bis(3-amidoquinolyl)diethylenetriamine-*N*,*N*',*N*''-triacetic acid (H_3DTPAAQ)

3-aminoquinone (0.323 g, 2.2 mmol) was added to the solution of DTPA-bis(anhydride) (0.400 g, 1.1 mmol) in dry DMF (20 mL). The reaction mixture was stirred for 5 h at 70 °C. The solvent was removed under reduced pressure and bright yellow colour product was obtained. The compound was washed with acetonitrile (3x10 mL) and diethyl ether (3x10 mL) three times and was dissolved in 5 ml water and was adjusted to pH 6 by dropwise addition of NaOH. The aqueous phase was washed with chloroform (3x10 mL). Water was then evaporated completely in vacuo and dried in vacuum overnight to afford a bright yellow powder product (yield: 0.650 g, 90%). ESI-MS in CH_3OH (*m/z*): $[M+H]^+$ calcd. for $C_{32}H_{35}N_7O_8$: 646.26 (100%). Found: 646.25 (100%). ^{1}H-NMR (500 MHz, Methanol-d_3) δ ppm: 2.86 (4H, s), 2.99 (4H, s), 3.66 (6H, s), 3.74 (4H, s), 7.39 -7.46 (3H, m), 7.46 - 7.56 (3H, m), 7.60 (4H, d), 7.71 (3H, d), 8.53 (2H, d), 8.86 (2H, d). FT-IR (KBr pellet, ν_{max}, cm^{-1}): 3260 (w), 1667(s, $\nu_{C=O}$ of COOH), 1608 (s, $\nu_{C=O}$ of CONH), 1558 (m), 1491(w), 1468 (s), 1384 (m), 1368 (m), 1286 (m), 1220 (w), 1093 (m), 991 (m), 902 (s), 783 (m). (vs, very strong; s, strong; m, medium; w, weak; br, broad). UV-vis (DMF, 298 K), λ_{max}, nm (ε, M^{-1} cm^{-1}): 265 (15,500), 318 (7000) and 331 (7000).

Synthesis of [Ln(DTPAAQ)(DMF)] (1-3) [Ln = Pr^{III} (1), Eu^{III} (2), Tb^{III}(3)]

The complexes **1**-**3** were prepared by following a general synthetic procedure. To a 5 mL MeOH solution containing 0.23 mmol of respective lanthanide salt [$Pr(NO_3)_3{\cdot}6H_2O$ (0.101 g), $Eu(NO_3)_3{\cdot}6H_2O$ (0.103 g), $TbCl_3{\cdot}6H_2O$ (0.100 g)] was added dropwise to an aqueous solution (10 mL) of H_3DTPAAQ (0.150 g, 0.23 mmol) pretreated with NaOH (0.027 g, 0.67 mmol) for 10 min. The reaction mixture was stirred at 40 ^{0}C for 3 h to obtain a light yellowish precipitate. The precipitate was filtered and washed successively with cold methanol (3 x 5 mL) and diethyl ether (3 x 5 mL) and finally dried in a vacuum over P_4O_{10} [yield: ~80%]. Diffraction quality crystals of complexes **1a**, **1**-**3** were grown from layering of Et_2O onto a DMF solution of the complexes at RT. The characterization data for the complexes are given below.

[Pr(DTPAAQ)(DMF)] (1). Yield: 0.203 g (81%). Anal. Calcd for $C_{35}H_{39}N_8O_9Pr$: C, 49.07; H, 4.59; N, 13.08. Found: C, 49.02; H, 4.46; N, 13.15. ESI-MS in DMF (*m/z*): $[M\text{-DMF} + H]^+$ calcd. for $C_{32}H_{32}N_7O_8Pr$ (relative abundance): 784.14 (100.0%), 785.14 (37.93%), 786.14 (8.5%). Found: 784.14 (100.0%), 785.14 (39.82%), 786.14 (7.8%). FT-IR (KBr pellet, ν_{max}, cm^{-1}): 3408 (w), 1609 (s, ν_{asym} CO_2^-), 1588 (s, $\nu_{C=O}$ of CONH), 1496 (m), 1466 (m), 1388 (s, $\nu_{sym}CO_2^-$), 1350 (m), 1293 (m), 1089 (m), 913 (m), 865 (m), 782.87 (s). UV-vis (DMF, 298 K), λ_{max}, nm (ε, M^{-1} cm^{-1}): 263 (10,200), 318 (5,000), 331(5,200). Molar conductivity in 10% aqueous DMF at 298 K [Λ_M /Scm^2mol^{-1}]: 13.6.

[Eu(DTPAAQ)(DMF)] (2). Yield: 0.180 g (75%). Anal. Calcd for $C_{35}H_{39}N_8O_9Eu$: C, 48.45; H, 4.53; N, 12.91. Found: C, 48.22; H, 4.32; N, 12.78. ESI-MS in DMF (m/z): $[M\text{-DMF} + H]^+$ calcd. for $C_{32}H_{32}N_7O_8Eu$ (relative abundance): 795.15 (100.0%), 794.15 (38.2%), 796.15 (45.5%), 797.15 (3.3%). Found: 795.15 (100.0%), 794.15 (90.8%), 796.16 (36.1%), 797.15 (7.8%). FTIR (KBr pellet, ν_{max}, cm^{-1}): 3431 (w), 1607 (s, ν_{asym} CO_2^-), 1589 (s, $\nu_{C=O}$ of CONH), 1496 (m), 1468 (m), 1388 (s, ν_{sym} CO_2^-), 1350 (m), 1294 (m), 1091 (m), 914 (m), 870 (m), 784 (s). UV-vis (DMF, 298 K), λ_{max}, nm (ε, M^{-1} cm^{-1}): 263 (17,300), 318 (5,040), 331 (5,020). Molar conductivity in 10% aqueous DMF at 298 K [Λ_M /Scm^2mol^{-1}]: 11.8.

[Tb(DTPAAQ)(DMF)](3). Yield: 0.195 g (78%). Anal. Calcd for $C_{35}H_{39}N_8O_9Tb$: C, 48.06; H, 4.49; N, 12.81. Found: C, 48.12; H, 4.35; N, 12.68. ESI-MS in DMF (*m/z*): $[M\text{–DMF+H}]^+$ calcd. for $C_{32}H_{32}N_7O_8Tb$ (relative abundance): 802.15 (100.0%), 803.15 (35.3%), 804.15 (8.5%). Found: 802.15 (100.0%), 803.15 (37.5%), 804.15 (7.5%). FTIR (KBr pellet, ν_{max}, cm^{-1}) 3425 (w), 1609 (s, ν_{asym} CO_2^-), 1589 (s, $\nu_{C=O}$ of CONH), 1496 (m), 1469 (m), 1387 (s, $\nu_{sym}CO_2^-$), 1350 (s), 1294 (m), 1093 (m), 913 (m), 872 (m), 783 (s). UV-vis (DMF, 298 K), λ_{max}, nm (ε, M^{-1} cm^{-1}): 263 (13,000), 318 (6,000) and 331 (7,000). Molar conductivity in 10% aqueous DMF at 298 K [Λ_M/Scm^2mol^{-1}]: 17.2.

X-ray crystallographic procedure

X-ray quality single crystals of complexes **1**-**3** were obtained by layering of diethyl ether on to a DMF solution of the complexes. Single-crystals of suitable dimensions were mounted on a glass fiber and used for data collection. All geometric and intensity data were collected on a Bruker D8 Quest Microfocus X-Ray CCD diffractometer equipped with an Oxford Instruments low-temperature attachment, with graphite-monochromated Mo Kα radiation (λ = 0.71073 Å) using ω-scan technique (width of 0.5° per frame) at a scan speed of 10 s per frame. Intensity data, collected using ω-2θ scan mode, were then corrected for Lorentz-polarization and absorption effects.[42] The structures were subsequently solved by direct methods using SHELXS-97[43] and was refined on F^2 by full-matrix least-squares technique using the SHELXTL 6.14 software package. The structures were further refined and processed with the SHELXL-97 incorporated into the WinGX 1.70 crystallographic package. All the hydrogen atoms were included in idealized positions and refined using a riding model. All non-hydrogen atoms were refined anisotropically. Perspective views of the complexes were obtained using ORTEP.[44] The CCDC deposition numbers for the complexes are 1033642 (**1a**), 1402443 (**1**), 1033643 (**2**) and 1402444 (**3**) respectively. These data can be obtained free of charge from

The Cambridge Crystallographic Data Centre via http://www.ccdc.cam.ac.uk/data_request/cif.

DNA binding experiments

DNA binding experiment was carried out in Tris- HCl/NaCl buffer (5mM Tris-HCl/NaCl, pH 7.2) using DMF solution of the complexes **1-3**. CT-DNA in the buffer medium gave the ratio of 1.9: 1 of absorbance in UV region at wavelength 260 and 280 nm which showed that DNA is free from protein. The concentration of DNA was calculated using known molar extinction coefficient at 260 nm (ε_{260} = 6600 $M^{-1}cm^{-1}$).[45] Absorption spectral titrations were performed by varying the concentration of CT-DNA while keeping the complex concentration constant. Due to the corrections made for the absorbance of CT-DNA itself. The equilibrium binding constant (K_b) of the complexes was determined by the following equation [32]

$[DNA]/(\varepsilon_a - \varepsilon_f) = [DNA]/(\varepsilon_b - \varepsilon_f) + 1/K_b(\varepsilon_b - \varepsilon_f)$

where [DNA] is the concentration of CT DNA in the base pairs, ε_a is the apparent extinction coefficient, ε_f and ε_b refers to the extinction coefficients of the complex in its free and fully bound form. The K_b values are obtained from the [DNA]/(ε_a - ε_f) *vs.* [DNA] plots.

Protein binding experiments

The interaction of the complexes **1- 3** with bovine serum albumin (BSA) has been studied from tryptophan emission-quenching experiments. The complex solutions were continuously added to the solution of BSA (2 μM) in 5 mM Tris-HCl-NaCl buffer (pH 7.2) and the quenching of the emission signals at 340 nm (λ_{ex} = 295 nm) were recorded. The quenching constant (K_{BSA}) has been determined quantitatively by using Stern-Volmer equation.[35] Stern-Volmer I_0/I vs. [complex] plots were made using the corrected fluorescence data taking into account the effect of dilution. Linear fit of the data using the equation: $I_0/I = 1 + K_{BSA}[Q]$, where I_0 and I are the emission intensities of BSA in the absence of quencher and in the presence of quencher of concentration [Q], gave the quenching constants (K_{BSA}).

DNA cleavage experiments

The photocleavage of SC pUC19 DNA (30 μM, 0.2 μg, 2686 base pairs) in presence of complexes was performed in Tris-HCl/NaCl buffer (50 mM, pH 7.2) by photo-irradiation of the samples with UV-A light of 312 nm (8 W) by agarose gel electrophoresis. Mechanistic studies were performed using different additives as ROS scavengers/quenchers (NaN_3, 200 μM; KI, 200 μM; L-histidine, 200 μM; DMSO, 2 μL; catalase, 4 units) prior to the addition of the complexes. To investigate the effect of D_2O on DNA photocleavage, D_2O was added for dilution of the sample to 20 μL. After incubation of the sample for 1 h in dark and quenched by gel loading dye, solution was loaded on 1% agarose gel having 1 μg/mL ethidium bromide. Electrophoresis was run for 2.0 h at 60 V in Tris-acetate EDTA (TAE) buffer in dark room. The quantification of cleavage products was performed using UVITEC Fire Reader V4 gel documentation system and UVI band software. The error observed in measuring the band intensities was in the range of 4-7%.

Cell cytotoxicity assay

The cytotoxicity of the complexes **2** and **3** was studied in HeLa cells using MTT assay which is based on the ability of mitochondrial dehydrogenases of viable cells to cleave the tetrazolium rings of MTT forming dark purple membrane impermeable crystals of formazan that could be measured at 540 nm after dissolving in DMSO.[19b] Approximately, $1x10^4$ cells were plated in 96 wells culture plate in Dulbecco's Modified Eagle Medium (DMEM) containing 10% FBS (10% DMEM) and after overnight incubation at 37 °C in a CO_2 incubator, various concentrations of the complexes dissolved in 1% DMSO were added to the cells and incubation was continued for 8 h in dark. For photocytotoxicity measurements, the culture plate was exposed to UV-A light of 365 nm (0.55 J cm^{-2}) for 30 min. The medium was then replaced with fresh DMEM-FBS and incubation was continued for further 20 h in dark. Finally, 25 μL of 4 mg mL^{-1} of MTT solution in PBS was added to each well and again incubated for an additional 3 h. After discarding the media, 200 μL of DMSO was added to dissolve the formazan crystals formed, and the absorbance at 540 nm was measured using a BIORAD ELISA plate reader. The cytotoxicity was measured from the absorbance ratio of the treated cells and untreated controls. The IC_{50} values were determined by non-linear regression analysis using GraphPad Prism software.

Cellular internalization by fluorescence microscopy

HeLa cells (4 x 10^4 cells/mm^2), plated on cover slips, were incubated with 150 μM of complexes **2** and **3** for 8 h in the dark, fixed with 4% paraformaldehyde for 10 min at 25 ^{0}C and washed with PBS. This was followed by staining with Hoechst 33342 for 10 min at 25 ^{0}C. The cells were washed, mounted in 90% glycerol solution containing Mowiol, an anti-fade reagent, and sealed. Images were acquired using Apotome.2 fluorescence microscope (Carl Zeiss, Germany) using an oil immersion lens at 63X magnification. The images were analyzed using the AxioVision Rel 4.8.2 (Carl Zeiss, Germany) software.

Conclusions

In summary, we presented a systematic investigation on a new series of stable lanthanide complexes having DTPA-bisamide aminoquinoline as octadentate chelating ligand containing 3-aminoquinoline as a fluorophore based remote sensitizer. The structural studies for complexes [Ln(DTPAAQ)(DMF)] (**1**-**3**) shows presence of nine-coordinate $\{LnN_3O_6\}$ core with distorted tricapped trigonal prismatic geometry around Ln(III). The Eu(III) and Tb(III) complexes show strong red and green lanthanide based emission when excited at quinoline-based chromophore respectively. This suggest efficient transfer of excited state energy from the remote antenna moiety to the embedded Eu(III) and Tb(III) ions for $^5D_0 \rightarrow {}^7F_J$ and $^5D_4 \rightarrow {}^7F_J$ *f-f* transitions respectively with long excited state lifetimes in milliseconds. The hairpin-shaped complexes shows efficient binding propensity with CT-DNA via partial intercalation through planar quinoline moieties with favourable stacking interactions with planar nucleobases. Moreover, we have also

observed significant enhancement of lanthanide based luminescence intensity upon interaction with CT-DNA in aqueous buffer medium. The [Ln(DTPAAQ)(DMF)] (**1**-**3**) complexes having a photoactive quinoline moiety display efficient UV-A light induced DNA cleavage activity involving formation of singlet oxygen ($^1O_2$) and hydroxyl radical ($^{\bullet}OH$) as the reactive species via type-II and photoredox pathways. Eu and Tb-complexes were photocytotoxic under UV-A light while remain nontoxic in the dark. Such spatio-temporal control is significant in serving dual purpose of imaging the cancer cell and remaining inactive within the cells in dark and become cytotoxic on photo-irradiation damaging the tumor. The cellular internalization studies of luminescent Eu(III) and Tb(III) complexes by confocal fluorescence microscopy using HeLa cells reveals primarily cytosolic localization of the complexes in cancer cells which remain viable, thus making the complexes potential for cellular imaging agent. The present results are of importance and hold promise towards designing and developing multimodal photoactive luminescent lanthanide complexes as sensing or theranostic agents. We are currently investigating prospects for the use of these luminescent constructs as potential carrier for chemotherapeutic drugs or other biologically active species.

Acknowledgements

We thank Science and Engineering Research Board (SERB), Government of India and IIT Kanpur for financial support. K.S. thank the Council of Scientific and Industrial Research (CSIR), S. B. thank IISc Bangalore for research fellowships. We are thankful to Prof. A. A. Karande, IISc, Bangalore, for her help in fluorescence microscopy.

Notes and references

1 Cotton in *Lanthanides and actinides,* McMillan Physical Science Series, McMillan Education, London, 1991.
2 (a) J.-C. G. Bünzli, *Chem. Rev.*, 2010, **110**, 2729-2755; (b) J.-C. G. Bünzli and S. V. Eliseeva, *Chem. Sci.*, 2013, **4**, 1939-1949.
3 (a) M. C. Heffern, L. M. Matosziuk and T. J. Meade, *Chem. Rev.*, 2014, **114**, 4496-4539; (b) A. J. Amoroso and S. J. A. Pope, *Chem. Soc. Rev.*, 2015, **44**, 4723-4742.
4 E. J. New, A. Congreve and D. Parker, *Chem. Sci.*, 2010, **1**, 111-118.
5 E. G. Moore, A. P. S. Samuel and K. N. Raymond, *Acc. Chem. Res.*, 2009, **42**, 542-552.
6 (a) A. Thibon and V. C. Pierre, *Anal. Bioanal. Chem*., 2009, **394**, 107-120; (b) K. Hanaoka, K. Kikuchi, S. Kobayashi and T. Nagano, *J. Am. Chem. Soc.*, 2007, **129**, 13502-13509.
7 (a) J. L. Major and T. J. Meade, *Acc. Chem. Res.*, 2009, **42**, 893-903; (b) M. Bottrill, L. Kwok and N. J. Long, *Chem. Soc. Rev.*, 2006, **35**, 557-571; (c) E. J. Werner, A. Datta, C. J. Jocher and K. N. Raymond, *Angew. Chem. Int. Ed.*, 2008, **47**, 8568-8580.
8 (a) P. Caravan, J. J. Ellison, T. J. McMurry and R. B. Lauffer, *Chem. Rev.* 1999, **99**, 2293-2352; (b) P. Caravan, *Chem. Soc. Rev*., 2006, **35**, 512-523.
9 S. J. Butler, L. Lamarque, R. Pal and D. Parker, *Chem. Sci.*, 2014, **5**, 1750-1756.
10 (a) S. J. Butler and D. Parker, *Chem. Soc. Rev.*, 2013, **42**, 1652-1666; (b) T. Gunnlaugsson and J. P. Leonard, *Chem. Commun*., 2005, 3114-3131.
11 (a) E. J. New, D. Parker, D. G. Smith and J. W. Walton, *Curr. Opin. Chem. Biol.*, 2010, **14**, 238-246; (b) Y. Ma, Y. Wang, *Coord. Chem. Rev*., 2010, **254**, 972-990.
12 Z. Liu, Z. Guo, *Chem. Soc. Rev*., 2013, **42**, 1568-1600.
13 M. L. P. Reddy, V. Divya and R. Pavithran, *Dalton Trans.*, 2013, **42**, 15249-15262.
14 (a) X. Wang, X. Wang, Y. Wang and Z. Guo, *Chem. Commun.*, 2011, **47**, 8127-8129; (b) X. Wang, X. Wang, S. Cui, Y. Wang, G. Chen and Z. Guo, *Chem. Sci*., 2013, **4**, 3748-3752.
15 R. Bonnett, *Chemical Aspects of Photodynamic Therapy*, Gordon & Breach: London, U. K. 2000.
16 M. Ethirajan, Y. Chen, P. Joshi and R. K. Pandey, *Chem. Soc. Rev*., 2011, **40**, 340-362.
17 K. E. Erkkila, D. T, Odom and J. K. Barton, *Chem. Rev*., 1999, **99**, 2777-2796.
18 (a) P. M. Bradley, A. M. Angeles-Boza, K. R. Dunbar and C. Turro, *Inorg. Chem.*, 2004, **43**, 2450- 2452; (b) H. T. Chifotides and K. R. Dunbar, *Acc. Chem. Res.*, 2005, **38**, 146-156.
19 (a) U. Basu, I. Pant, I. Khan, A. Hussain, P. Kondaiah and A. R. Chakravarty, *Chem. Asian J.*, 2014, **9**, 2494-2505; (b) S. Banerjee, P. Prasad, A. Hussain, I. Khan, P. Kondaiah and A. R. Chakravarty, *Chem. Commun.*, 2012, **48**, 7702-7704.
20 (a) J. S. Butler, J. A. Woods, N. J. Farrer, M. E. Newton and P. J. Sadler, *J. Am. Chem. Soc.*, 2012, **134**, 16508−16511.
21 (a) A. K. Patra, T. Bhowmick, S. Roy, S. Ramakumar and A. R. Chakravarty, *Inorg. Chem*., 2009, **48**, 2932-2943; (b) A. K. Patra, T. Bhowmick, S. Ramakumar, M. Nethaji and A. R. Chakravarty, *Dalton Trans*., 2008, 6966-6976; (c) A. K. Patra, M. Nethaji and A. R. Chakravarty, *Dalton Trans*., 2005, 2798-2804.
22 J. L. Sessler and R. A. Miller, *Biochem. Pharmacol.*, 2000, **59**, 733-739.
23 (a) A. Hussain and A. R. Chakravarty, *J. Chem. Sci.*, 2012, **124**, 1327-1342; (b) A. Hussain, D. Lahiri, M. S. A. Begum, S. Saha, R. Majumdar, R. R. Dighe and A. R. Chakravarty, *Inorg. Chem.*, 2010, **49**, 4036-4045; (c) A. Hussain, K. Somyajit, B. Banik, S. Banerjee, G. Nagaraju and A. R. Chakravarty, *Dalton Trans*., 2013, **42**, 182-195.
24 S. Dasari and A. K. Patra, *Dalton Trans.* 2015, DOI: 10.1039/c5dt02852c.
25 (a) T. Gunnlaugsson and D. Parker, *Chem. Commun.,* 1998, 511-512; (b) T. Gunnlaugsson, D. A. MacDónail and D. Parker, *Chem. Commun*., 2000, 93-94; (c) T. Gunnlaugsson, D. A. MacDónail and D. Parker, *J. Am. Chem. Soc*., 2001, **123**, 12866-12876. (d) T. Gunnlaugsson, *Tet. Lett*., 2001, **42**, 8901-8905; (e) C. P. McCoy, F. Stomeo, S. E. Plush and T. Gunnlaugsson, *Chem. Mater.*, 2006, **18**, 4336-4343; (f) L. J. Govenlock, J. A. K. Howard, J. M. Moloney, D. Parker, R. D. Peacock and G. Siligardi, *J. Chem. Soc., Perkin Trans. 2*, 1999, 2415-2418.
26 (a) E. Debroye, S. V. Eliseeva, S. Laurent, L. V. Elst, S. Petoud, R. N. Muller and T. N. Parac-Vogt, *Eur. J. Inorg. Chem*., 2013, 2629-2639; (b) D. J. Lewis, F. Moretta, T. Hollooway and Z. Pikramenou, *Dalton Trans*., 2012, **41**, 13138-13146; (c) Y. Kataoka, D. Paul, H. Miyake, T. Yaita, E. Miyoshi, H. Mori, S. Tsukamoto, H. Tatewaki, S. Shinoda and H. Tsukube, *Chem. Eur. J.*, 2008, **14**, 5258-5266; (d) M. E. Masaki, D. Paul, R. Nakamura, Y. Kataoka, S. Shinoda, H. Tsukube, *Tetrahedron*, 2009, **65**, 2525-2530.
27 (a) D. Parker, K. Pulukkody, F. C. Smith, A. Batsanov and J. A. K. Howard, *J. Chem. Soc., Dalton Trans*., 1994, 689-693; (b) D. Parker, R. S. Dickins, H. Puschmann, C. Crossl and J. A. K. Howard, *Chem. Rev.*, 2002, **102**, 1977-2010.

28 (a) M. S. Konings, W. C. Dow, D. B. Love, K. N. Reymond, S. C. Quay and S. M. Rocklage, *Inorg. Chem.*, 1990, **29**, 1488-1491; (b) S. Aime, F. Benetollo, G. Bombieri, S. Colla, M. Fasano and S. Paoletti, *Inorg. Chim. Acta*, 1997, **254**, 63-70
29 (a) G. Bobba, Y. Bretonnière and J.-C. Frias, *Org. Biomol. Chem*., 2003, **1**, 1870-1872; (b) R. A. Poole, G. Bobba, M. J. Cann, J.-C. Frias, D. Parker and R. D. Peacock, *Org. Biomol. Chem*., 2005, **3**, 1013-1024.
30 (a) W. D. Horrocks and Jr. D. R. Sudnick, *J. Am. Chem. Soc.*, 1979, **101**, 334-340; (b) A. Beeby, I. M. Clarkson, R. S. Dickins, S. Faulkner, D. Parker, L. Royle, A. S. de Sousa, J. A. G. Williams and M. Woods, *J. Chem. Soc. Perkin Trans.*, 1999, **2**, 493-504.
31 (a) T. M. Kelly, A. B. Tossi, D. J. McConnell and T. C. Strekas, *Nucleic Acid Res*., 1985, *13*, 6017-6034; (b) A. M. Pyle, J. P. Rehamann, R. Meshoyrer, C. V. Kumar, N. J. Turro and J. K. Barton, *J. Am. Chem. Soc.*, 1989, **111**, 3051-3058.
32 A. Wolfe, G. H. Shimer and Jr. T. Meehan, *Biochemistry*, 1987, **26**, 6392-6396.
33 P. B. Glover, P. R. Ashton, L. J. Childs, A. Rodger, M. Kercher, R. M. Williams, L. De Cola and Z. Pikramenou, *J. Am. Chem. Soc.*, 2003, **125**, 9918-9919.
34 M. Lee, A. L. Rhodes, M. D. Wyatt, S. Forrow and J. A. Hartley, *Biochemistry*, 1993, **32**, 4237-4245.
35 J. R. Lakowicz, *Principles of Fluorescence Spectroscopy,* 3rd ed. Springer: New York, 2006.
36 Y.-Q. Wang, H.-M. Zhang, G.-C. Zhang, W.-H. Tao and S.-H. Tang, *J. Lumin*., 2007, **126**, 211-218.
37 D. Costa, H. D. Burrows and da Gracüa Miguel, *Langmuir*, 2005, **21**, 10492-10496.
38 (a) S. Gupta, S. Mondal, A. Mhamane and A. Datta, *Inorg. Chem.,* 2013, **52**, 12314-12316; (b) S. Bakthavatsalam, A. Sarkar, A. Rakshit, S. Jain, A. Kumar and A. Datta, *Chem. Commun*., 2015, **51**, 2605-2608.
39 (a) M. C. DeRosa and R. J. Crutchley, *Coord. Chem. Rev.*, 2002, **233-234**, 351-371; (b) K. Szaciłowski, W. Macyk, A. Drzewiecka-Matuszek, M. Brindell, and G. Stochel, *Chem. Rev*., 2005, **105**, 2647-2694.
40 A. U. Khan, *J. Phys. Chem*., 1976, **80**, 2219-2228.
41 D. D. Perrin, W. L. F. Armarego and D. R. Perrin, *Purification of Laboratory Chemicals*, Pergamon Press, Oxford, 1980.
42 N. Walker and D. Stuart, *Acta Crystallogr. A.*, 1983, **39**, 158.
43 G. M. Sheldrick, SHELX-97, Program for Refinement of Crystal Structures, University of Göttingen, Göttingen, Germany, 1997.
44 M. N. Burnett and C. K. Johnson, ORTEP-III, Report ORNL - 6895; Oak Ridge National Laboratory: Oak Ridge, TN, 1996.
45 M. E. Reichmann, S. A. Rice, C. A. Thomas and P. Doty, *J. Am. Chem. Soc.*, 1954, **76**, 3047-3053.

Graphical Abstract for Table of Contents

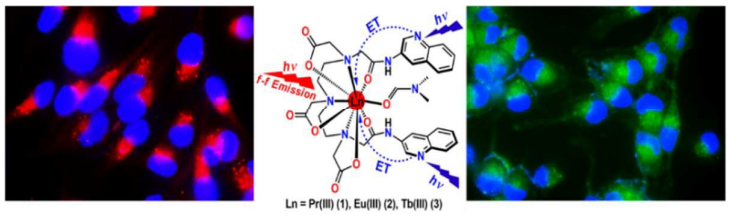

This work presents a systematic study of luminescent Lanthanide(III) complexes, [Ln(DTPAAQ)(DMF)] where (Ln(III) = Pr (**1**), Eu (**2**), Tb (**3**), H_3DTPAAQ=*N,N''*-bis(3-amidoquinolyl)diethylenetriamine-*N,N',N''*-triacetic acid for their crystal structures, luminescent properties, binding interactions with DNA and protein, photo-induced DNA cleavage, remarkable photocytotoxicity, cellular internalization studies. The findings are of importance and hold promise towards developing multimodal photoactive luminescent lanthanide complexes as therapeutic, bioimaging, or theranostic agents.